J Solid State Electrochem (2011) 15:1297–1315
DOI 10.1007/s10008-011-1372-1

REVIEW

Thirty years of platinum single crystal electrochemistry

V. Climent · Juan M. Feliu

Received: 18 February 2011 / Revised: 25 February 2011 / Accepted: 28 February 2011 / Published online: 12 April 2011

Abstract The electrochemistry of platinum single crystals is historically reviewed. After a brief revision of historical results dating before the publication of the landmark experiment by J. Clavilier of the flame annealing in 1980, the controversy introduced by this experiment into the surface electrochemistry community is described. Questions about the structure and composition of the platinum surface after the flame annealing and their implications on the characteristic voltammetry of platinum single crystal electrodes were slowly answered in the years that followed the first introduction of this methodology. One of the last questions to be solved was that about the nature of the chemical species responsible for the charge transfer process that leads to the so-called unusual features in the voltammogram. This was solved with the charge displacement experiment. Nowadays, a great deal of knowledge has been gathered about the structure of the interphase between platinum electrodes and electrolytic solutions and also about the electrocatalytic behaviour of platinum surfaces. State-of-the-art information about platinum electrochemistry is provided, with emphasis on results from our group, especially those obtained with a thermodynamic analysis, involving either constant or variable temperatures and with the laser-induced temperature jump method.

Keywords Platinum single crystal · Flame annealing · Potential of zero charge · Adsorption · Surface structure

V. Climent · J. M. Feliu (✉)
Institute of Electrochemistry, University of Alicante,
Ap 99,
03080 Alicante, Spain
e-mail: juan.feliu@ua.es

Introduction

From kinetic gas theory, it is well-known that, assuming unity sticking coefficient, a surface will be fully covered by gas molecules in one second provided that the gas partial pressure would be 10^{-6} torr [1]. This means that any solid electrode in the laboratory atmosphere is, at least partially, contaminated by unknown impurities. This was a great drawback for the use of solid electrodes, and methods to

obtain reproducible results in the different laboratories had to be developed in order to use these materials with the same confidence as it was possible with mercury electrodes and so progress in the understanding on the problems that could be addressed from different laboratories using complementary experimental techniques. In this report, we will address the case of platinum, a material with important reactivity as electrocatalyst.

The plan of the paper is centred on the impact of the flame annealing experiment, although a first section in which the state-of-the-art of the electrochemical characterisation of polycrystalline and single crystalline platinum electrodes is included because this strongly conditioned further interpretations of the experimental results. In a first part, the proper handling and topography of the single crystal electrode surfaces is discussed. Then, the problem of the chemical species involved in the charge transfer is explicitly addressed. Once these problems are solved, thermodynamic information on the interphase can be extracted, as done in the more recent physical electrochemistry studies. References are selected to guide readers in the main lines of understanding and cannot be considered as exhaustive, especially the earlier ones.

Before the flame annealing

A general consensus was reached in the 1970s on the behaviour of several solid electrodes, also including Pt: After continuous potential cycling between the onset of hydrogen and oxygen evolution, the voltammetric profile was stable and defined a characteristic shape, reproducible in all laboratories worldwide [2–5]. This characteristic response was established in dilute sulphuric acid, usually 0.5 M, because it was a clean enough acid electrolyte, stable in the whole potential range. It involved three potential regions (Fig. 1). In the first one, two couples of reversible adsorption processes merged in the potential range between 0.4 V vs. RHE and the beginning of hydrogen evolution. The charge transfer was assigned to hydrogen adsorption and desorption and attributed to the underpotential deposition (UPD) of a full hydrogen monolayer in the negative-going sweep and to the release of protons in the positive-going sweep. Due to energetic considerations, the most positive peaks (H_s, 0.27 V vs. RHE) were considered to be due to the deposition of strongly adsorbed hydrogen atoms while the less positive peaks (H_w, 0.12 V vs. RHE) would correspond to weakly adsorbed hydrogen. A third peak was also observed in the positive-going sweep (0.22 V vs. RHE), and it was claimed to be only observed with clean surfaces. The charge under the H UPD peaks was taken as 210 μC/cm^2, and this was a tool to normalize the real surface area of the different platinum samples [6].

Thus, an initially contaminated platinum surface that had a low ability to adsorb hydrogen (and also to evolve or oxidize hydrogen) showed an increasing amount of charge in this H UPD region with successive potential cycling until a constant value was reached. In this moment, the characteristic voltammetric response was observed, as shown in Fig. 1, irrespective of the initial state of the surface: The final 'activated' voltammetric profile required more or less cycles to be reached, depending on the initial

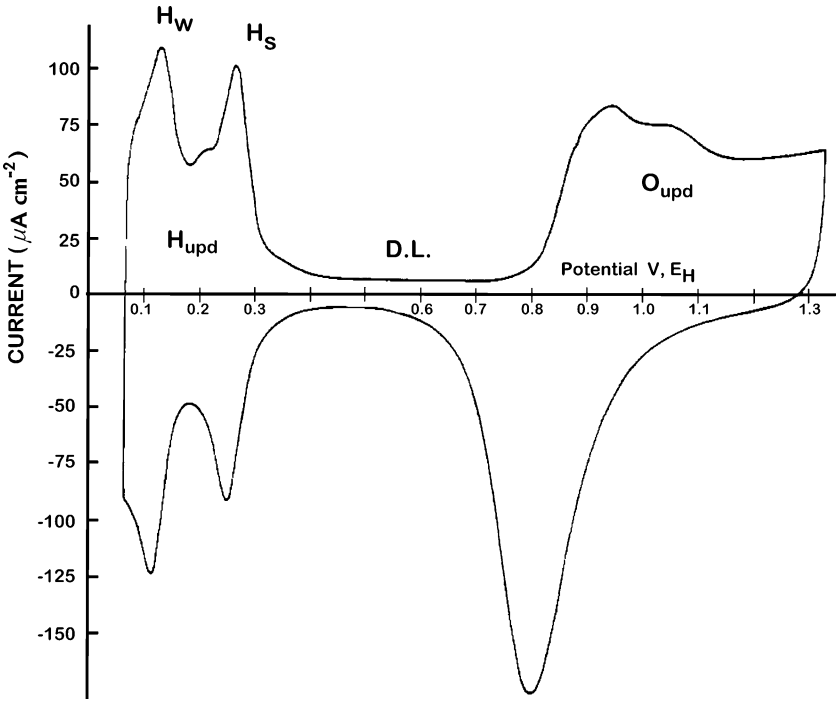

Fig. 1 Cyclic voltammogram for a polycrystalline platinum electrode in 0.5 M H_2SO_4 solution. Sweep rate 50 mV/s (adapted with permission from Conway et al. [3])

amount of surface impurities, mainly carbon-containing molecules or other classical poisons of platinum such as sulphur or arsenic, that also blocked the surface sites. Many cleaning procedures were checked [7], including flame heating, but the electrochemical activation was almost universally accepted in all laboratories, and the examination of the H UPD was considered a fingerprint of the clean polycrystalline Pt/sulphuric acid electrolyte interface.

Further, between 0.4 and 0.9 V vs. RHE, a featureless region with small current was observed and assigned to double layer charging. Solution impurities, such as heavy metal deposition [8], could contribute in this region, and the observation of electric current peaks in this potential range was characteristic of the presence of contributions due to contaminations, especially those present in the solution side.

At increasing potentials, between 0.9 V vs. RHE and the onset of oxygen evolution, a relatively flat oxidation process in which some peaks could be identified [2, 9] was counterparted by a single, bell-shaped, reduction process in the negative-going sweep. The asymmetry of this surface redox process, which involved a charge double than that in the H UPD region, was attributed to the formation/dissolution of a full monolayer of adsorbed oxygen before oxygen evolution, a sort of O UPD [2]. The presence of other contributions in this region or the difference between the oxidation and reduction charges were considered the result of surface contamination that disappeared with successive cycles, or required purification of the solution by pre-electrolysis, until the characteristic profile was attained, in a similar way as described for the H UPD region [3]. The irreversibility observed in the O UPD region was related to the value of the upper potential limit: If the sweep was reversed at a relatively low potential, say 1.0 V vs. RHE where the O UPD charge was only a small fraction of the maximum reached at the onset of oxygen evolution, the reduction process was faster and the voltammogram looked more symmetrical. This behaviour lead Brian Conway to propose that the oxygenated species generated on the surface (supposedly to be mainly OH) could penetrate into the metallic network and exchange its position at the surface with Pt atoms underneath [2]. As the upper limit, or time, increased, the first oxygen-containing species would evolve to adsorbed O atoms that also could penetrate into the metallic structure [10]. Then, the place exchange would take place more and more intensively, and because of this penetration into the bulk, the oxygenated species (finally a full PtO monolayer) would require lower potentials to be reduced, compared to the potential required to its formation on the 'bare' Pt surface.

An alternative interpretation of these well-defined and reproducible voltammetric profile was proposed for the H UPD zone: Instead of two energetically different states of H adsorption that would be filled consecutively on a uniform surface, the first one being finished at a particular intermediate coverage and the second one completing the full adlayer, the presence of the two peaks would reflect surface heterogeneity. This means that the couple of peaks at 0.27 V vs. RHE would reflect complete H monolayer adsorption on a particular type of site and the second one would also correspond to the interaction of hydrogen atoms at full monolayer coverage, but on sites of different symmetry and consequently of different adsorption energy. To check this interpretation, F.G. Will proposed the use of single crystal electrodes with Miller indices corresponding to the Pt basal planes, Pt(111), Pt(100) and Pt(110) [11]. The Pt atoms arranged in different unit cells would interact at different energies with the hydrogen atom, due to the different type and overlapping between the electronic local density of a site (metal orbitals or dangling bonds) and the adsorbed hydrogen.

The relevant surfaces were isolated by sealing into lime glass, and it was clear that the surfaces were initially contaminated. Following the method used for polycrystalline Pt, the electrodes were activated by electrochemical cycling. As a result (Fig. 2), it was observed that the strongly adsorbed hydrogen peak was particularly related to the Pt(100) orientation and the weakly adsorbed hydrogen peak was mainly observed with Pt(110) and also Pt(111). This latter orientation was also considered the main source of the third peak observed in the positive-going sweep, which required special care in solution cleanliness. In this way, surface heterogeneity was considered to be responsible of the adsorption states present in the voltammogram of

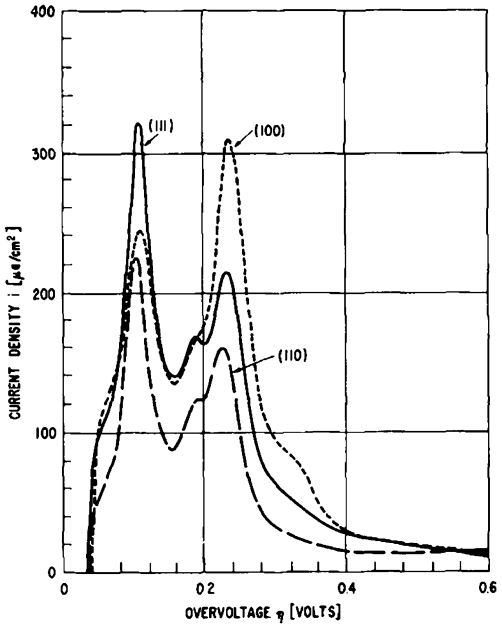

Fig. 2 Cyclic voltammograms for platinum single crystal faces (100), (111) and (110) at 25 °C. Sweep rate 0.1 V/s (reprinted with permission from: Will [11])

the polycrystalline samples. At this early stage, it was already pointed out that some surface damage could be associated to the cleaning treatment because measured hydrogen charges would lead to abnormally high saturation coverage and consequently more careful experiments, avoiding this traditional activation step should be carried out.

These experiments required the use of ultra-high vacuum (UHV) methodology, and only few selected laboratories were able to afford the required equipment [12–18]. The idea was to characterise the surfaces in UHV, mainly by using low energy electron diffraction (LEED) to assess the surface order, and Auger electron spectroscopy (AES) to check surface cleanliness, especially the absence of carbon impurities. Once characterised in UHV, the single crystal electrodes with well-defined surfaces had to be transferred to another chamber in which the electrochemical experiment, namely cyclic voltammetry, could be carried out at normal pressure and ambient temperature. The electrode/solution interface was made by using the dipping procedure, avoiding any sealing material [19]. In spite of the especial care and the expertise of the research groups involved in the experiment, reported results were not coincident. In addition, charge densities for H adsorption were usually much lower than those expected, especially for Pt(111), in comparison with those calculated by considering a process involving one electron per surface platinum atom, well-known from the unit cell of the electrode used [13, 15, 16, 18].

Flame annealing

The situation changed dramatically with the publication of the voltammetric profiles for the different single crystal electrodes obtained after the flame annealing treatment [20–23] by J. Clavilier and R. Durand. The underlying hypothesis was that the single crystals, once prepared, would keep their surface order, but their surfaces were contaminated. To eliminate the impurities, the well-known catalytic properties of platinum to oxidize organic molecules at high temperature in the presence of oxygen were assumed. In this way, the as-prepared well-ordered electrodes were considered to be clean after heating in a gas-oxygen flame at ≈1.300 °C. To avoid surface contamination of the surface during the transfer from the flame to the cell through the laboratory atmosphere, the samples were quenched with water while still at a relatively high temperature. The temperature dropped and the surfaces were protected by a remaining droplet of water attached to the electrode that would difficult the arrival of gaseous impurities to the surface. Once in the cell, the protective water droplet could be dispersed in the whole solution volume, and thus, the surface impurities would remain at trace level. As in UHV studies, the contact between the electrode and the solution was made by using the meniscus arrangement, to avoid the necessity of covering the sides of the electrode with other material that could decompose at high temperature [19].

The voltammograms were found to be structure sensitive, and the peak at 0.12 V vs. RHE was definitely assigned to adsorption at (110) sites and that at 0.27 V vs. RHE to adsorption at (100) sites (Fig. 3). Moreover, their charge density values were compatible with full hydrogen coverage in all orientations, and the profiles changed with the composition of the electrolyte solution, pointing out specific adsorption effects (Fig. 4).

The most surprising result was that some features were never observed previously with polycrystalline samples. This was specially noted with the Pt(111) orientation that showed the so-called unusual states at relatively high potentials, especially in perchloric acid, in which specific anion adsorption was expected to be small, as deduced with other metals. The voltammograms were stable, provided that the potential range explored was kept between the onset of hydrogen evolution and the upper end of the ‘double layer’

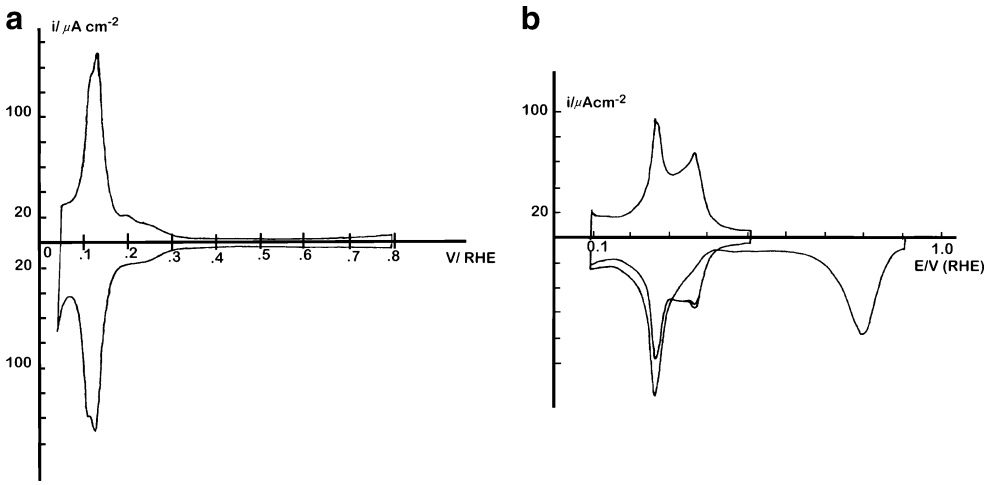

Fig. 3 Historic cyclic voltammograms published for the first time for flame annealed electrodes for the (110) (**a**) and (100) (**b**) crystallographic directions. Sweep rate 50 mV/s (reprinted with permission from Clavilier et al. [20, 22])

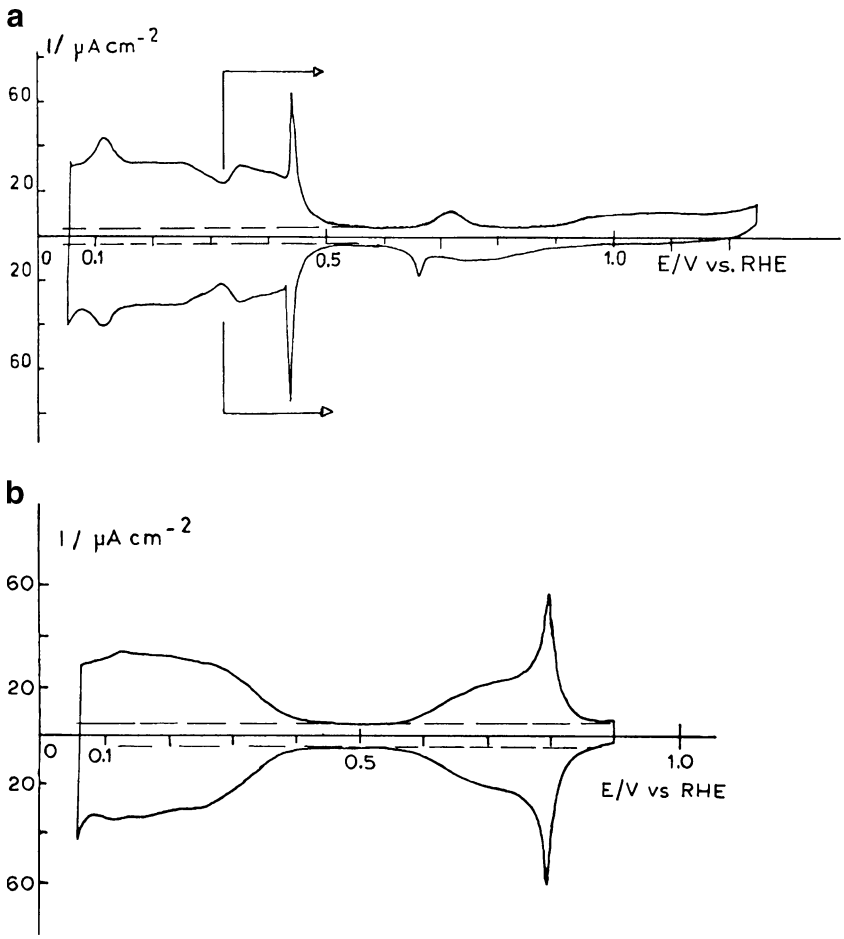

Fig. 4 Historic cyclic voltammograms published for the first time for flame annealed electrodes for the (111) crystallographic direction. Sweep rate 50 mV/s. **a** 0.5 M H_2SO_4, **b** 0.1 M $HClO_4$ (reprinted with permission from Clavilier [21])

region as defined in each electrode in a similar way as in polycrystalline electrodes, e.g. prior to the beginning of adsorption of oxygenated species. Interestingly, strong modification of the voltammograms was noticed after increasing the upper potential limit of the sweep [20]. The resulting voltammograms after such oxidation led to profiles with adsorption states more similar to those observed on activated polycrystalline electrodes. It is noteworthy that the H UPD voltammetric profile of Pt(111) in sulphuric acid after first oxygen adsorption/desorption at high coverage was quite similar to that reported after UHV-electrochemistry experiments in which also a small number of activation cycles was included in the pretreatment [24].

The first question that arose after the publication of these results was related to the possible existence of a surface contamination. It could happen that the voltammetric profiles would reflect the presence in solution of a metallic impurity that could be underpotentially deposited, and then the origin of the anomalous profile of the Pt(111), the so-called butterfly, could be due to adatoms other than hydrogen. In order to eliminate this possibility, the experimental results should be reproduced in other laboratories and, preferentially, under different sample preparation conditions. The first one was reported by P.N. Ross in a Meeting held in Logan in 1982, and the corresponding paper was published in the following year [25].The electrode was characterised in UHV and then transferred successfully to the electrochemical chamber. The voltammetry of Pt(111) in hydrofluoric acid electrolyte was reasonably similar to that reported after flame annealing in perchloric acid.

Another important contribution came from C.N. Reilley at Chapel Hill where the flame annealing–water quenching was reproduced successfully as well as the voltammetric modifications after cycling in the O UPD region [26–28]. A hydrogen flame was used and the quenching step was done in water containing hydrogen, instead of air. This also led to noticeable modifications in the voltammetric profile, notably that of Pt(100) as it was already observed [23, 26]. After cooling in reductive atmosphere, the main H UPD state shifted to 0.37 V vs. RHE. The state at 0.27 V vs. RHE was obtained after cooling in air or after some cycles in the O UPD region. As time passed, more and more laboratories reported the same results, and thus, the possibility of UPD processes other than those related to the species nominally present in the electrolyte solution progressively vanished to definitely disappear in the mid-1980s.

Topography

A question that was immediately asked dealt with the topography of the surface after (a) flame annealing and (b) after O UPD cycles. It was questioned whether the flame annealed electrodes, suddenly quenched by water from a very high to the ambient temperature, could be disordered and whether the voltammetric feature could represent that of a sort of frozen state in which the surface Pt atoms were not in their equilibrium positions. Under this hypothesis, O UPD cycles would increase the surface mobility of the atoms on these unstable positions in such a way that they could reach a more stable final position. Thus, the voltammetric profile changes would represent the modification of the surface to attain a flat, stable situation that would correspond to the nominal orientation defined by the corresponding Miller index. In this respect, it was shown in an extensive series of papers that the fast potential cycling with different sweep limits was able to produce final voltammetric profiles similar to those obtained from Pt(111) and Pt(100) electrodes subjected to few oxygen adsorption cycles [29, 30]. The surface modification was undergone on polycrystalline Pt samples and is perfectly reproducible. It was suggested that fast dissolution–re-deposition of platinum atoms were able to create stable surfaces in which the interaction of the surface atoms was particularly favourable.

Indirect evidences about the surface topography were initially collected. First of all, successful UHV-electrochemistry transfer experiments in which the quality of the final voltammograms was similar to that obtained with the flame annealing procedure were reported [25, 31, 32]. Among them, it is worth mentioning one particular procedure that involved characterisation of the Pt(111) electrode in the UHV chamber, followed by iodine dosing, resulting in a iodine layer with a $\left(\sqrt{7} \times \sqrt{7}\right)\mathrm{R}19.1^0$ structure, as well-known in surface science studies[33]. With this protective layer, the single crystal was transferred to the electrochemical chamber, where a solution of CO was used to displace the iodine layer at low temperature, fully covering the surface, again preventing the adsorption of other possible impurities. Finally, the CO adlayer was stripped out voltammetrically, in a perchloric acid test solution free of CO. As the stripping process does not require high potentials, the electrode integrity was preserved. It was found that the voltammetric profile after stripping was the same as after flame annealing. A similar method was also applied without the UHV requirement, by annealing the electrode through resistive heating in an iodine atmosphere. In this way, the quenching step necessary in the flame annealing methodology was avoided [34].

In another work, the quality of the electrode after potential cycling in the oxide region was tested with the UHV approach [35]. In this experiment, the electrode was prepared and characterised in UHV by LEED and AES. Then, the electrode was transferred to the electrochemical cell and a voltammogram similar to that obtained with the flame annealing, in sulphuric acid, was successfully recorded. Next, the electrode was oxidized and reduced several times, and its voltammetric profile changed accordingly. The surface with the modified voltammogram was then successfully transferred back to the UHV chamber, without impurities from the solution, and the LEED pattern was consistent with that expected from a disordered surface. Other indirect evidences were also gained from the evolution of the voltammetric profiles of the basal planes as a consequence of the introduction of surface steps of different symmetry [36–40]. In this respect, it was found that, in order to obtain results consistent with the hard sphere model of the surface, the flame annealing had to be followed by water quenching in absence of oxygen, especifically under reductive atmosphere. If not, the voltammetry of the basal planes, with the only exception of Pt(111), was more similar to those obtained with stepped surfaces, and the stepped surfaces themselves would indicate the presence of more surface sites that those expected from its nominal orientation. Quantitative charge analysis will be discussed below.

The direct evidence was finally gained by using in situ STM [41]. Figure 5 summarizes this result. The experiment was made in a natural (111) facet of a single crystal bead and pointed out that a single sweep adsorption of oxygen at full coverage was enough to evidence a fully disordered surface after oxide reduction. This disordering took place through a place exchange mechanism as earlier proposed for activated polycrystalline electrodes although in a different experimental situation [10]. Incidentally, there was no doubt that the bead contained flat (111) facets after flame annealing because they could be identified in the surface of the bead at the positions required for a fcc crystal. Moreover, in an experiment published at the 33rd ISE Meeting [42], the voltammetry of the natural facets of the Pt single crystal beads was presented and shown to be consistent to that reported for the corresponding single crystals after flame annealing. STM studies were extended to other orientations, and surface disorder as a consequence of oxygen adsorption was considered to be a general rule [43–48]. Thus, the activation procedure, albeit being successful in cleaning the surface from contamination, leads to disordered surfaces, the only exception being heavily stepped surfaces such as Pt(210) [44]. Nowadays, consistent STM results have been reported for many single crystal electrodes under different surface pretreatments, and a good correlation between the voltammetric response and the surface topography has been firmly established in all cases studied [48–50]. Other experiments were based in

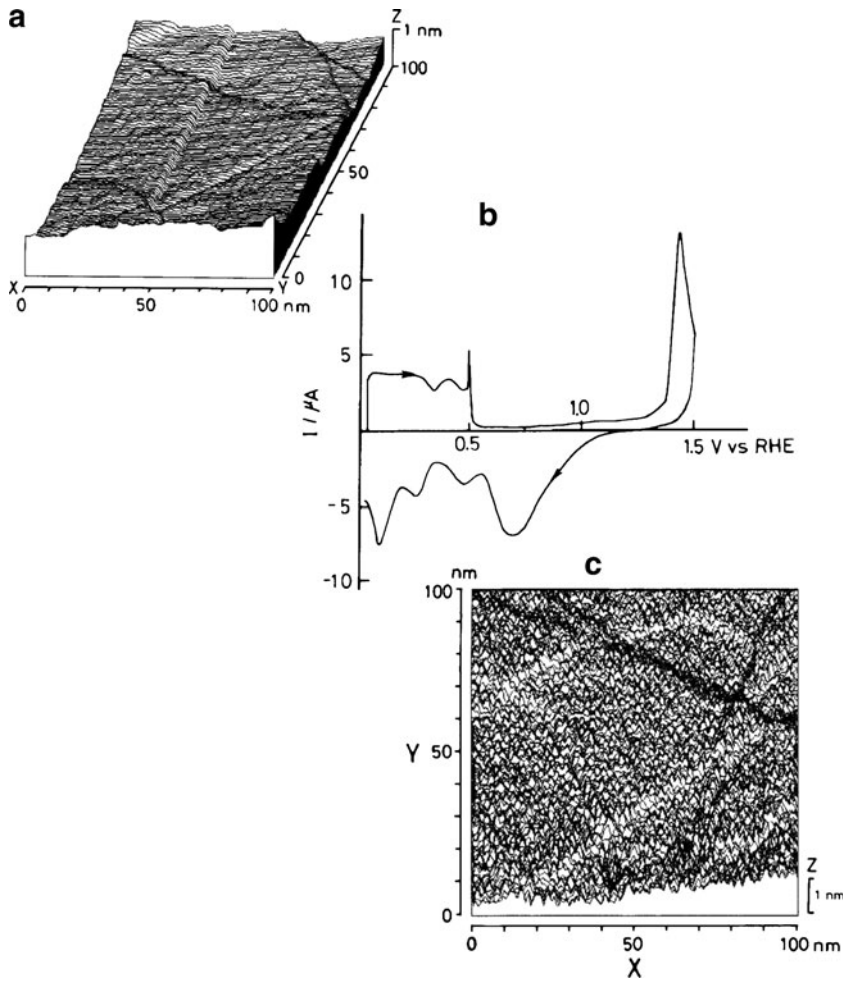

Fig. 5 STM study of the effect of potential cycling in the oxide formation region on the structure of a Pt(111) electrode in 0.05 M H_2SO_4. **a** STM image of a Pt(111) facet surface at 0.95 V vs RHE. Tip potential was 0.90 V vs RHE. The tunnelling current was 2 nA. Scan speed was 200 nm/s. **b** Cyclic voltammogram of a Pt(111) electrode in 0.05 M H_2SO_4. Sweep rate 50 mV s^{-1}. **c** STM image obtained after five potential cycles between 1.5 and 0.05 V RHE, under the same conditions as **a** (reprinted with permission from Itaya et al. [41])

UHV characterisation, mainly with the Pt(100) electrode [51, 52]. As a consequence, the conclusion that voltammetry can be confidently used as a surface characterisation technique of Pt electrodes can be reached. The only surface pole that remains elusive is Pt(110) and its vicinal surfaces, whose electrochemical responses have not been completely understood yet in relation to its surface topography [53]. The situation is complicated because of the well-known (2×1) reconstruction of Pt(110) that has been widely studied in UHV [54] and pointed out in several reports [55, 56].

Finally, it should be remarked that quenching at deliberately high temperatures could lead to some surface disorder [57]. Thus, the possibility to obtain surfaces with different topography by flame annealing–fast water quenching is possible, although it was not the case if some few seconds are elapsed after heating the electrode. Conversely, more careful heating treatments, using controlled temperature and atmosphere, have been recently described that can be applied to platinum. It is expected that the quality of the surfaces would improve although the limiting step would be perhaps the quality of surface polishing [58–62].

The problem of the chemical nature of the adsorbing species

Even after the general consensus described above was achieved about the validity of the flame annealing methodology to prepare well-ordered and clean surfaces in electrochemical environment, a strong debate remained about the nature of the electrochemical processes that give place to the unusual voltammetric features observed at high potentials. Once it was accepted that they were due to adsorption of species present in the electrolyte, and not to a contamination or to structural defects created during the annealing in the flame, only three possible hypotheses remained to explain these features: (a) hydronium adsorption to form adsorbed hydrogen, (b) hydroxyl adsorption from water dissociation and (c) specific adsorption of anions. This debate was mainly focused on Pt(111) although it has implications for all platinum surfaces, including the polycrystalline one.

In favour of hypothesis (a) was the coincidence of the charge integrated in the whole potential range with the amount calculated from the hard sphere model of the

surface, assuming one electron per platinum atom. For Pt (111), this charge was similar for different electrolytes (perchloric, sulphuric, phosphoric and acetic acid solution) and very close to the 241 μC/cm^2 calculated with the hard sphere model (Fig. 4). The most important argument against this hypothesis was the exceedingly high energy that would be associated to hydronium reduction to justify its adsorption at such high potentials ($\Delta G^0 = -n$FE for reaction $H_2 \leftrightarrows 2H_{ads}$ would range between −100 and −160 kJ/mol for $0.5 < E < 0.8$ V vs. RHE) in comparison with the reported values for hydrogen adsorption in UHV (42 kJ/mol) [35]. In this regard, strong stabilization of the adsorbed hydrogen in electrochemical environment by the interaction with the water was argued in favour of hypothesis (a) [63]. One argument in favour of hypothesis (c) was the similarity of the voltammetric profile obtained for Au (111), a metal that is well-known to possess very low capacity to adsorb hydrogen.

The first result that gave strong support against the hypothesis of hydrogen adsorption at high potentials was given in 1986 and consisted in a detailed study of the dependence of the unusual states on the sulphate concentration and pH [64]. In this work, it was proved that the unusual states in sulphuric acid shift with sulphuric acid concentration but remain invariant after the pH is changed. This is a clear indication of the participation of sulphate in this process. Moreover, if hydrogen adsorption took place in this potential range, a shift of the voltammetric features close to 60 mV/pH unit would be observed.

Conversely, unusual states in perchloric acid shifted with pH but remained invariant with perchlorate concentration. This proves that the peak observed in perchloric acid is of different nature that the peak observed in sulphuric acid, although this experiment alone cannot distinguish between H reductive adsorption or OH oxidative adsorption. What this result seems to rule out is the participation of anion adsorption in this process, such as perchlorate or fluoride adsorption. The similarity between the voltammogram measured in perchloric and fluorhydric acid [25, 65] (and more recently in trifluoromethyl sulphonic acid [66]) suggests that other species, common to all these electrolytes, is at the origin of this process.

As indicated above, one of the arguments in favour of hydrogen adsorption was the coincidence of the voltammetric charge with the value calculated with the hard sphere model. To pursue this argument further, Clavilier and coworkers studied the effect of the introduction of steps on the Pt(111) surface on the corresponding voltammetric response [37–39, 63]. This analysis demonstrated that the coincidence between the charge integrated in the voltammogram and that calculated theoretically extends beyond the basal (111) plane to its vicinal surfaces. Figure 6 shows the positive sweep for Pt(S)[n(111)×(111)] stepped surfaces in 0.1 M H_2SO_4. It is clear that the peak at 0.12 V vs. RHE, initially absent on the flat (111) surface, grows as the step density increases. This observation gives confidence in the assignment of this peak to the voltammetric contribution of step sites. For the charge analysis, the voltammetric contribution of the steps can be easily separated from the terrace contributions taking a reasonable base line for the integration, as shown in the inset of Fig. 6. Step charges integrated in this way agree quite well with one electron per step atom and are the same for different electrolyte solution compositions. This is taken as an indication that these adsorption processes correspond to hydrogen adsorption on step sites. The integration of the terrace contribution requires more assumptions. First, both usual and unusual contributions were integrated together. Second, total charge was integrated without considering any double layer correction to subtract the capacitive contribution to the

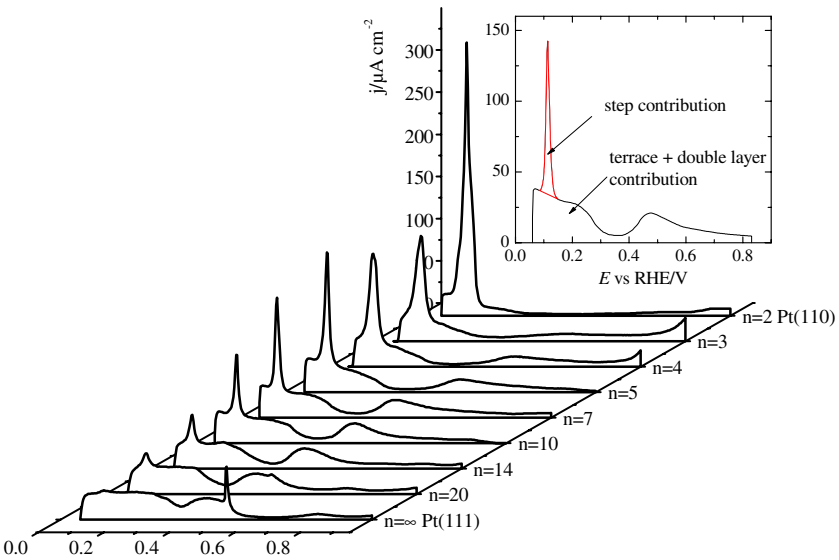

Fig. 6 Cyclic voltammograms corresponding to Pt(S)[n(111)×(111)] stepped surfaces in 0.1 M H_2SO_4. Sweep rate: 50 mV/s. *Inset* shows the separation of the two contributions corresponding to terrace and step sites, for the Pt(775)

interfacial charge. The corresponding area integrated under these assumptions is also indicated in the inset of Fig. 6. The plot of such charges versus the density of steps gives straight lines whose slope is related with the overall number of electrons transferred per platinum atoms involved in the processes under study. This is shown in Fig. 7, where charges are plotted as function of $1/(n-2/3)$ which is a magnitude proportional to the step density [37]. The result is consistent with one electron per platinum atom, reinforcing the idea that a single species is involved in the usual potential range between the onset of hydrogen evolution and the onset of platinum oxidation.

Another important conclusion that was obtained from the analysis described in the previous paragraph regards the double layer charge. Since the plot of the experimental terrace charges against the step density give a straight line with slope close to the theoretical value calculated from the hard sphere model and because these charges are integrated without double layer correction, it is deduced that double layer contribution must be approximately constant within the crystallographic zone. Otherwise, either a 'wrong' slope value would be obtained or no straight line would be obtained at all. The difference between the intercept with the *y*-axis (infinite terrace width) and the theoretical value of charge for Pt(111) allows to calculate the average double layer capacity for all the surfaces in the zone, being around 73 μF cm^{-2} [63].

More information could be gained from the coupling of non-electrochemical techniques to interrogate in situ the composition of the double layer. One of such approaches uses radioactive labelled anions, such as H_2 $^{35}SO_4$. It was demonstrated that sulphate increases its surface concentration associated to the unusual adsorption states [67]. Moreover, an estimation of the saturation coverage could be given [68].

The second non-electrochemical technique capable of shedding some light on this issue was infrared spectroscopy. Sulphate gives very distinctive vibrational bands. Subtraction of spectra collected above and below the onset of the unusual states gives bands corresponding to adsorbed species closely related with those characteristic of sulphate (or bisulphate) anions, but with slightly different vibrational frequencies. The variation of the vibrational frequency upon adsorption can be rationalized in terms of the electronic effect of the bonding with the surface. Although some ambiguity remains in the identification of the species (either sulphate or bisulphate) giving the vibrational bands, this experiment again gives evidence of the increase of sulphate species in the double layer associated with the unusual states [65, 69–74].

These experiments, while providing evidence of the participation of sulphate in the unusual states, do not indicate the nature of the species that is participating on the charge transfer process. In this way, competitive adsorption of hydrogen and sulphate species could lead to a situation where hydrogen desorption would be triggered by sulphate adsorption in a process where, although the hydrogen is the species storing the charge, it would be energetically linked to the presence of sulphate, i.e. its potential would depend on the sulphuric acid concentration. To solve this uncertainty, a new experiment was devised. The problem with the separation of the charges can be expressed in the

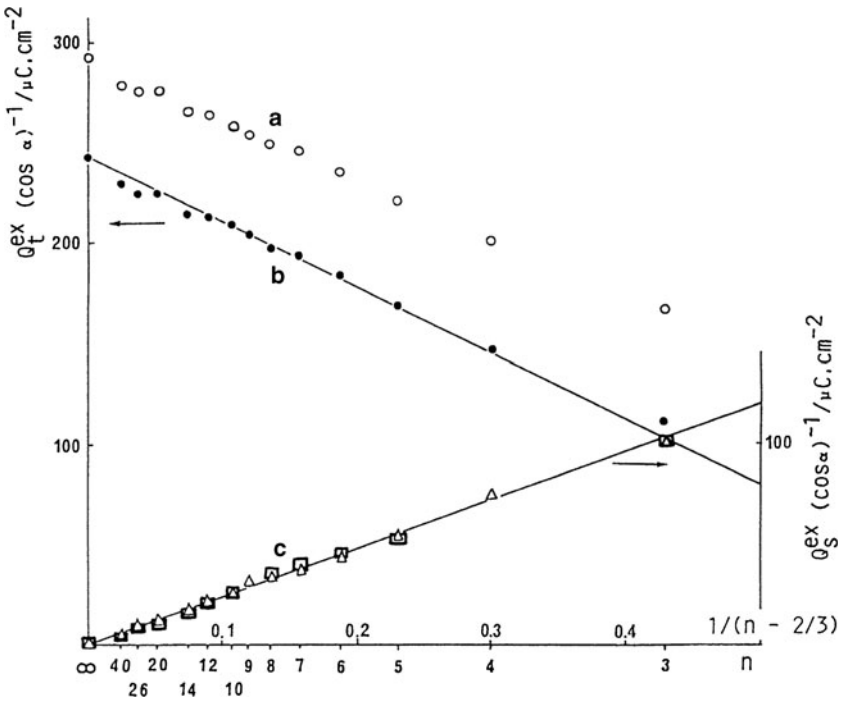

Fig. 7 Charge density for terrace (**a**, **b**) and step contribution (**c**) integrated in the voltammograms of Pt(S)[*n*(111)×(111)] stepped surfaces in 0.5 M H_2SO_4 (*circles* and *triangles*) and 0.1 M $HClO_4$ (*squares*), as a function of $1/(n-2/3)$. **a** corresponds to the raw integrated charge, while **b** is obtained after a constant double layer correction. Charges are divided by $\cos(\alpha)$ to project them on the plane of the terrace (reprinted with permission from Clavilier et al. [37])

following way: In the positive-going potential sweep, both desorption of hydrogen and adsorption of anion would contribute with positive currents. In the negative-going sweep, anion desorption and hydrogen adsorption both contribute with negative charges. An alternative way of expressing the problem is to say that voltammetry is a differential technique and an integration constant is necessary to extract absolute (i.e. non-relative) values of charge from the voltammetric currents. The charge displacement experiment implies using a substance that adsorbs sufficiently strong to force desorption of everything present on the surface. Now, desorption of hydrogen will give positive charges and desorption of anions will give negative charges. In this way, the electrical nature of the species adsorbed on the interphase can be identified. As displacing agent, CO [75–78] and I_2 [79] have been used, with the former being with difference the most convenient for the following reasons: (a) It can be easily removed from the solution, once the experiment is finished, by purging with an inert gas. (b) It can be stripped off the surface allowing checking that the surface has not suffered any irreversible modification during the displacement process. (c) There is a broad range of potentials, from the onset of hydrogen evolution to around 0.45 V vs. RHE, where CO can be adsorbed without further faradaic transformation (i.e. oxidation to CO_2).

The procedure for the CO charge displacement involves the introduction of CO in the gas atmosphere of the cell, while the electrode is held potentiostatically at a given potential value. The current is recorded during the displacement of the adsorbed species and the double layer charge present on the interphase at this potential. To complete the experiment, the excess CO from the solution can be purged by bubbling Ar and the degree of blockage of the surface can be voltammetrically checked. Finally, adsorbed CO can be oxidized to CO_2, which is a very clean reaction allowing the recovery of the initial state of the surface at the end of the experiment.

The results demonstrated that positive charges are displaced at potentials close to the hydrogen evolution reaction [75–78] while negative charges flow if the charge displacement is performed at a potential higher than the unusual states observed in sulphuric acid [76, 77]. Figure 8 exemplifies this result for the Pt(111) electrode. The maximum charge displaced in the hydrogen region depends on the crystallographic orientation of the electrode. For Pt (111), it amounts to 2/3 of the monolayer, meaning that the hydrogen adsorption does not saturate the surface. This experiment proofs that unusual states correspond to anion adsorption in sulphuric acid. Although the CO charge displacement cannot be performed at potentials higher than the unusual states in perchloric acid because CO oxidation would take place, negative charges are displaced at potentials in the double layer region, indicating the unusual states correspond also to anionic adsorption [75]. This point was further proved using iodine as a displacement agent [79].

The data obtained from the magnitude of the CO charge displacement can be further exploited with the introduction of few additional concepts [80, 81]. The charge that flows during the potentiostatic CO adsorption will equal the difference between the charge at the end of the process and that at the beginning.

$$q_{\mathrm{dis}} = q(E, \mathrm{CO}) - q(E) \tag{1}$$

If it is assumed that the charge on the CO covered surface is sufficiently small, it can be considered negligible in comparison with that initially present, and it can be assumed that the charge displaced equals the total charge present on the electrode surface at the potential of the experiment. The concept of total charge will be discussed below in more detail, but at this point, it is sufficient to know that total charge is all the charged stored in the interphase, including both the charge involved in adsorption processes and that capacitatively stored in the double layer that is called free charge. The total charge is the magnitude measured with the CO charge displacement experiment. It is negative at the onset of the hydrogen evolution reaction since hydrogen contributes almost exclusively to the total charge and becomes positive at high enough potentials. The potential where total charge is negligible can be considered the potential of zero total charge (pztc). This could be located by repeating the experiment at different potentials until a zero displacement transient is obtained or, what is more convenient, by obtaining a charge versus potential curve from the integration of the voltammogram using the displaced charge at a single (or several, if available) potential values as integration constant. This procedure is illustrated in Fig. 9, where the pztc can be located around 0.33 V vs. RHE as the intercept of the charge curve with the q=0 axis.

The notion of total charge has a straightforward application in coulometric measurements from stripping voltammetry. Let us use CO stripping as an example to illustrate this point. In fact, it was the discrepancy between the CO coverage calculated from the stripping voltammetry charge density and that calculated from spectroscopic measurements what served as inspiration for the CO displacement experiment. The difficulty in the coulometric calculation stems from the fact that after the stripping of adsorbed CO the total interfacial charge is recovered to the value corresponding to the clean surface. Therefore, the stripping charge includes both the charge for the oxidation of CO and the charge involved in the recovery of the interfacial charge [82]. Before the CO coverage can be calculated from the stripping charge, the charge involved in

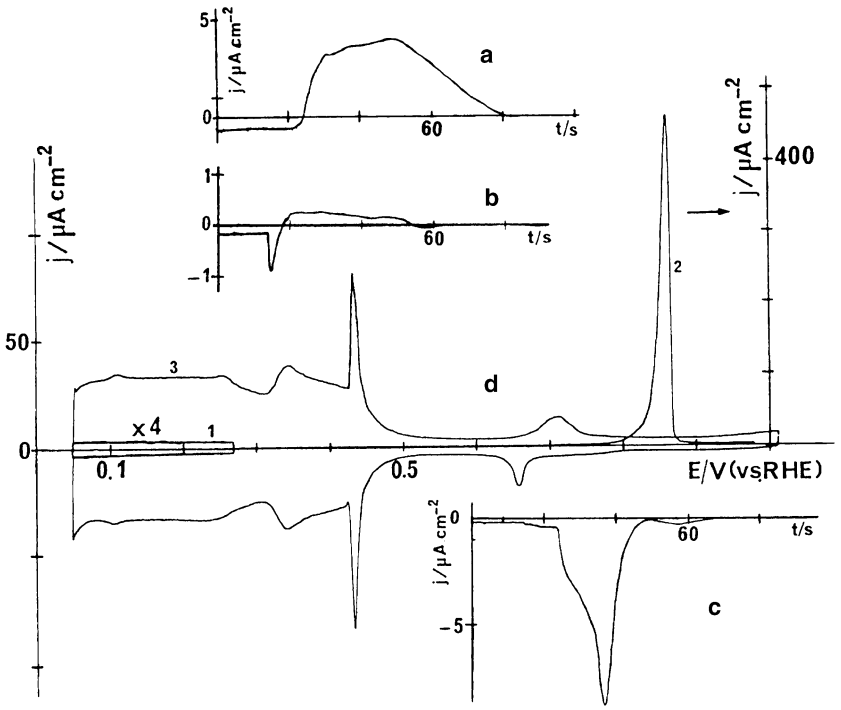

Fig. 8 **a**–**c** Current density–time transients corresponding to CO adsorption experiments on a well-ordered Pt(111) electrode in 0.5 M H_2SO_4 (E_{ads}= 0.08, 0.30 and 0.50 V vs RHE, respectively). **d** Voltammograms for the same electrode in the CO-free electrolyte, after CO adsorption: *1* control of the surface blocking by adsorbed CO (50 mV/s), *2* stripping of the adsorbed CO (20 mV/s) and *3* recovery of the initial voltammetric profile (50 mV/s; reprinted with permission from Feliu et al. [77])

the recovery of the interphase must be subtracted. This has been called double layer correction and involves not only double layer free charge, in the capacitive sense, but also charge involved in the readsorption of anions.

$$q = q_{\text{far}} + \left[q\left(E_{\text{up}}\right) - q(E, \text{CO})\right] \tag{2}$$

where q_{far} stands for the faradaic charge involved in the CO stripping, and the term in brackets represent the non-faradaic charge involved in the process which equals the difference between the total charge at the end and that at the beginning of the process. E and E_{up} stand for the lower and upper limit of the potential excursion. Since initially the electrode is covered with CO, $q(E, \text{CO})$ is very small and can be considered negligible, resulting the following equation

$$q_{\text{far}} = q - q\left(E_{\text{up}}\right) \tag{3}$$

where $q\left(E_{\text{up}}\right)$ can be calculated, as shown before, from the integration of the voltammogram and a single value of displaced charge, taken as an integration constant.

These notions can be used for any coulometric calculation, not only CO oxidation. Another example would be the reductive stripping of NO [83]. In this case, after elimination of an NO adlayer that takes place at potentials close to hydrogen evolution, the surface is covered with hydrogen. The charge from hydrogen readsorption needs to be taken into account to calculate the NO coverage from the stripping charge. The use of Eq. 2 for the case of CO is special since CO is also used in the calculation of the total charge through the charge displacement experiment. In this case, it can be demonstrated that Eq. 3 is exact and there is no need to neglect $q(E, \text{CO})$ since charge appears both in Eqs. 1 and 2 and both terms cancel out [84].

In this way, the classical H UPD states also contain anion contributions. This happens in all cases, irrespectively of the single crystal studied [76, 77, 85, 86]. It also happens with polycrystalline platinum samples and a direct consequence is that the classical charge density value used to normalize the real surface area has to be revised, as it has been recently pointed out [87].

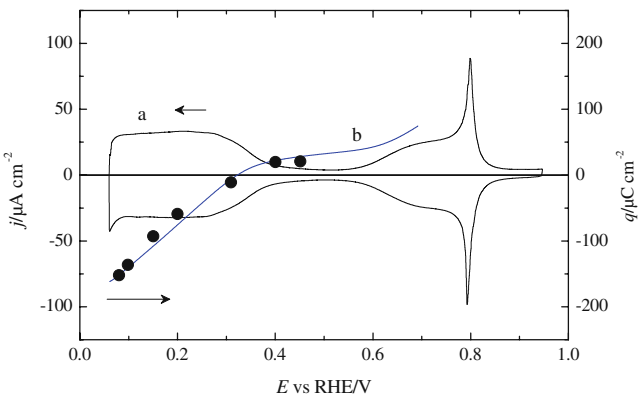

Fig. 9 **a** Cyclic voltammogram of a Pt(111) electrode in 0.1 M $HClO_4$, sweep rate=50 mV/s. **b** Charge integration from the cyclic voltammogram. The *circles* are the opposite of the displaced charges during the CO displacement experiment at different potentials

Thermodynamic analysis

The development of the field of interfacial electrochemistry has been intimately linked to the use of the electrocapillary equation. In the case of liquid electrodes, like mercury, the measurement of the surface tension has provided a great deal of information about the structure and composition of the double layer that led to the development of models for the interpretation of experimental results [88]. In the case of solid electrodes, the application of the electrocapillary equation has been questioned, since an additional term to consider the surface stress in addition to the surface tension should be taken into account. The estimation of the relative importance of this additional term suggests that it can be neglected, and in consequence, the same form of the electrocapillary equation is also valid for solid electrodes [89].

The application of the electrocapillary equation to study the interphase in contact with platinum electrodes has the additional complication of the existence of adsorption processes [90]. In the simplest case of the contact of a platinum electrode with a solution of a monoprotic acid whose anion can be adsorbed specifically, the interphase would be composed of the following species: Pt, e, H, H^+, A^-, A, H_2O, where H and A are the adsorbed forms of H^+ and A^-, respectively, with A^- being the anion corresponding to the acid present in the electrolyte. Therefore, the electrocapillary equation should be written as:

$$-\mathrm{d}\gamma = \sigma_M \mathrm{d}E + \Gamma_{H^+}\mathrm{d}\mu_{H^+} + \Gamma_H \mathrm{d}\mu_H + \Gamma_A \mathrm{d}\mu_A + \Gamma_{A^-}\mathrm{d}\mu_{A^-} \quad (4)$$

where γ is the surface tension, σ_M is the electronic charge density on the metal, Γ_i and μ_i are the surface excess, relative to water, and chemical potential of the species *i*. However, due to the existence of the following equilibriums, the different chemical potentials involved in Eq. 4 are not independent,

$$H^+ + e \rightleftarrows H \quad -F\mathrm{d}E = \mathrm{d}\mu_H - \mathrm{d}\mu_{H^+} \quad (5)$$

$$A^- \rightleftarrows A + e \quad F\mathrm{d}E = \mathrm{d}\mu_A - \mathrm{d}\mu_{A-} \quad (6)$$

Introduction of these dependences into Eq. 4 allows eliminating dependent terms, transforming the electrocapillary equation into:

$$-\mathrm{d}\gamma = (\sigma_M - F\Gamma_H + F\Gamma_A)\mathrm{d}E + (\Gamma_{H^+} + \Gamma_H)\mathrm{d}\mu_{H^+} + (\Gamma_A + \Gamma_{A^-})\mathrm{d}\mu_{A^-} \quad (7)$$

In this way, it is demonstrated that the electronic (also called free) charge, σ_M, and the surface excesses of adsorbed species cannot be determined independently with this approach. The term in brackets that multiply d*E* can only be determined as a whole, and it is called total charge (cf. above). This fact is reflecting the impossibility of distinguishing the actual position of the charges at the interphase with a macroscopically thermodynamic approach. This is illustrated schematically in Fig. 10, where two different models of the interphase would lead to identical determination of the total charge. Situation in Fig. 10b can be considered to be reached from Fig. 10a after an internal reorganization of the charges in the double layer that leads to the formation of a covalent bond between the surface and the proton. Such internal reorganization would not involve charge flow through the external circuit and therefore cannot be distinguished from a purely ionic bond with just the thermodynamic approach.

The application of the electrocapillary equation to study adsorption processes on platinum electrodes was pioneered by Lipkowski's group [91–102]. One of the systems that have been more deeply investigated with this approach is sulphate adsorption on Pt(111) and its vicinal surfaces [92, 93, 100–102]. Other systems studied are halide adsorption [96–98] and hydrogen and hydroxyl adsorption from perchloric acid solutions [94, 99]. The information obtained with this method includes surface excesses, electrosorption valencies and Gibbs energies of adsorption.

Equation 7 for the case of sulphate adsorption can be written:

$$-\mathrm{d}\gamma = Q\mathrm{d}E + (\Gamma_{H^+} + \Gamma_H)\mathrm{d}\mu_{H^+} + \left(\Gamma_{SO_4} + \Gamma_{SO_4^{2-}}\right)\mathrm{d}\mu_{SO_4^{2-}} + \left(\Gamma_{HSO_4} + \Gamma_{HSO_4^-}\right)\mathrm{d}\mu_{HSO_4^-} \quad (8)$$

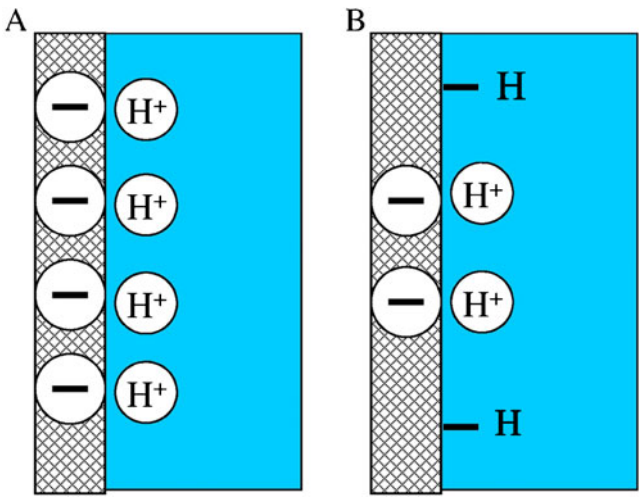

Fig. 10 Schematic representation of two different charge distributions at the interphase leading to the same total charge but with different hydrogen coverage

since both sulphate and bisulphate species are present in the solution and could be, in principle, adsorbed. In this case, the total charge is given by:

$$Q = \sigma_M - F\Gamma_H + 2F\Gamma_{SO_4} + F\Gamma_{HSO_4}$$

As before, the different chemical potentials in Eq. 8 are not independent but are linked through the acid–base equilibrium:

$$HSO_4^- \rightleftarrows H^+ + SO_4^{2-} \quad \mu_{HSO_4^-} = \mu_{H^+} + \mu_{SO_4^{2-}} \tag{9}$$

At constant pH and in the presence of an excess supporting electrolyte, it can be written:

$$d\mu_{HSO_4^-} = d\mu_{SO_4^{2-}} = RTd\ln(c_{sulf}) \tag{10}$$

where c_{sulf} stands for the total sulphate+bisulphate concentration. Under these conditions, Eq. 8 is reduced to:

$$-d\gamma = Q\,dE + \Gamma_- RTd\ln(c_{sulf}) \tag{11}$$

where Γ_- is the total surface excess of sulphate and bisulphate. The starting point for the analysis is a set of curves charge vs potential for a set of different concentrations. Integration of such curves would give the surface tension, up to an integration constant:

$$\gamma = -\int_{E^*}^{E} Q dE + \gamma(E^*) \tag{12}$$

E^* is chosen in such a way that the integration constant is common to all the concentrations. For the case of anion adsorption, that means that E^* is low enough and so the surface excess of the anion is negligible. The charge curves are usually obtained from the integration of the voltammogram. For this, knowledge of the pztc would be necessary, although it can be demonstrated that this is not necessary if the integration constant of the voltammogram is common for all the concentrations [97].

Then, the surface excesses can be calculated according to:

$$\Gamma = -\frac{1}{RT}\left(\frac{\partial\gamma}{\partial\ln(c_{sulf})}\right)_Q \tag{13}$$

Alternatively, the independent variable can be changed from the potential to the charge with the use of the Legendre transformation of Eq. 11 and the introduction of Parsons function ($\xi = \gamma + QE$). It has been shown that the use of charge is more appropriate, leading to less mathematical artefacts in the mathematical analysis of the data.

Figure 11B shows a set of data showing the variation of sulphate surface excess obtained with this approach. Interestingly, the curve shows two plateaus. Sulphate adsorption starts at E>0.3 V vs. RHE, rising slowly at the beginning, being followed by a steep increase associated with the sharp spike in the voltammogram. After this spike, a plateau close to 2.5×10^{14} ions/cm^2 is attained. If the potential is further increased, a new rise in sulphate concentration takes place and a maximum surface excess of 3×10^{14} ions/cm^2 is attained.

As discussed previously, sulphate adsorption on Pt (111) has become a benchmark system and extensive work has been done to characterise it with the maximum definition. Apart from the purely electrochemical data just mentioned, this system has been investigated with other non-electrochemical techniques such as radiotracers [67, 68], infrared spectroscopy [65, 69–74, 103] and STM [104, 105]. Among them, STM results deserve further mention here in connection with the results of the thermodynamic analysis. For this system, an ordered overlayer has been described with periodicity ($\sqrt{3} \times \sqrt{7}$). This adlayer is composed of (bi)sulphate ions adsorbed with the C_3 axis perpendicular to the surface and three oxygen atoms bonding to corresponding platinum atoms and chains of water and/or hydronium species between them. Incidentally, the same structure has been observed for sulphate adsorption on the (111) plane of other fcc metals, such as gold [106], palladium [107, 108] and rhodium [109]. This adlayer has been imaged at potentials located between the spike and the small adsorption process between 0.6 and 0.8 V vs. RHE. The coverage corresponding to this structure is 0.2 sulphate ions per platinum atom. This value should be compared with the result obtained with the thermodynamic analysis, since it coincides with the coverage attained in the second plateau, at higher potentials (the atomic density of platinum on the (111) surface is 1.5×10^{15} atoms/cm^2). However, in the potential range where this adlayer has been observed, the coverage obtained through the thermodynamic analysis is ca. 16% smaller since the coverage consistent with the STM image in only obtained in the second plateau. To explain this inconsistency between both results, the existence of different rotational domains on the sulphate adlayers with unmatching domain borders has been proposed to explain the existence of the first plateau with smaller coverage than the one corresponding to the ideal, perfectly ordered ($\sqrt{3} \times \sqrt{7}$) structure [110, 111]. Such rotational domains are indeed observed in the STM image [104]. Under this hypothesis, the small peak observed at high potentials in the voltammogram corresponding to Pt(111) in H_2SO_4 solutions would be due to the reorganization of the rotational domains to obtain bigger domains with less domain borders and, consequently, higher sulphate coverage. Unfortunately, such reorganization has not been observed with STM and the ordered ($\sqrt{3} \times \sqrt{7}$) structure disappear at high potentials [105]. Therefore, the adscription of the peaks at high potentials in the voltammogram of Pt(111) in sulphuric acid solutions is still controversial [112]. Still,

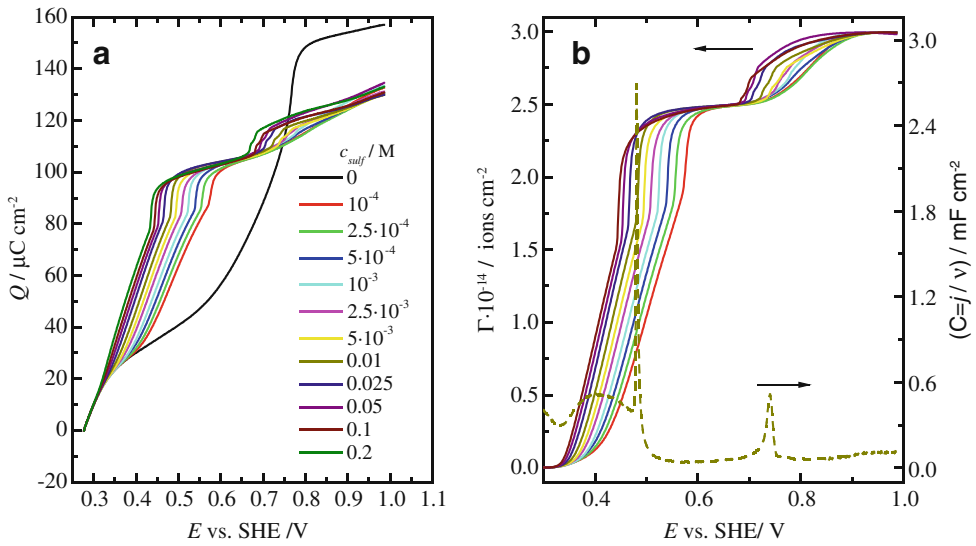

Fig. 11 **a** Charge curves integrated from cyclic voltammograms recorded for a Pt(111) electrode in 0.1 M $HClO_4$ solution with different H_2SO_4 concentration, as indicated in the graph. **b** Total sulphate surface excess calculated from the thermodynamic analysis based on the electrocapillary equation applied to the charge curves in **a**. The *dashed line* represents the pseudocapacity obtained for the Pt(111) electrode in 0.1 M $HClO_4$+0.01 M H_2SO_4

any hypothesis to explain this process should take into account the experimental facts obtained with the thermodynamic analysis, namely the potential of the process shift with sulphate concentration but not with pH variation [101, 110] and sulphate surface excess sharply increases in this potential region. OH adsorption as the only process producing this peak, as suggested in [112], is not consistent with these experimental facts.

Temperature dependence of the voltammograms

Temperature is undoubtedly among the most important variables in physical chemistry. Unfortunately, in electrochemistry, it has to compete in importance with the electrode potential and many times it has been relegated to a second place. This is especially true in the case of interfacial electrochemistry, where the number of studies that use the temperature to extract additional information is relatively limited. The first studies that used temperature variation in interfacial electrochemistry date back to the classical studies based on mercury electrodes [113–116]. In this case, the analysis of the results was based on the electrocapillary equation. In the extension of these studies to solid electrodes stand out the works of A. Hamelin and F. Silva with gold electrodes [117–120]. The extension to platinum electrodes was hampered by the conceptual difficulty associated to the existence of adsorption processes and the duality between the notions of free and the total charges. The first study of the temperature dependence of the process of hydrogen adsorption on polycrystalline platinum used well-established concepts of the thermodynamic of electrochemical cells to extract the entropy of adsorption of hydrogen from the peak potential variation with the temperature [121]. The application of these concepts to single crystal electrodes was pioneered by G. Jerkiewicz, who introduced the concept of a generalized isotherm into the analysis [122–125]. This approach will be briefly discussed below.

The global reaction for hydrogen adsorption, when the reaction taking place in the RHE is also considered, is:

$$1/2H_2 + e^w \rightleftarrows H_{ads} + e^r \tag{14}$$

where e^w and e^r represent the electrons in the working and reference electrodes, respectively. Application of the thermodynamic equilibrium condition to this reaction leads to the following generalized isotherm:

$$\frac{\theta}{1-\theta} = \sqrt{f_{H_2}} \exp\left(\frac{-\Delta\overline{G}^{f}_{H_{ads}/H_2} - FE}{RT}\right) \tag{15}$$

where the term $\Delta\overline{G}^{f}_{H_{ads}/H_2}$ is a formal Gibbs energy whose dependence with coverage accounts for all deviations of the real isotherm from the Langmurian behaviour. $\Delta\overline{G}^{f}_{H_{ads}/H_2}$ can be calculated from Eq. 15 and a set of data of hydrogen coverage as a function of electrode potential, as obtained from the integration of the voltammetric currents. From this, the standard value of $\Delta\overline{G}^{0}_{H_{ads}/H_2}$ can be obtained from the extrapolation to zero coverage. $\Delta\overline{S}^{0}_{H_{ads}/H_2}$ can be obtained from:

$$\Delta\overline{S}^{0}_{H_{ads}/H_2} = -\frac{d\Delta\overline{G}^{0}_{H_{ads}/H_2}}{dT} \tag{16}$$

From the entropy of the global reaction (Eq. 14) and the tabulated value of the entropy of H_2, the entropy of adsorbed hydrogen can be calculated as:

$$\overline{S}^{0}_{H} = \Delta\overline{S}^{0}_{H_{ads}/H_2} - \frac{1}{2}\overline{S}^{0}_{H_2} \tag{17}$$

Analogous reactions can be written for the entropy of adsorbed OH.

$$H_2O \rightleftarrows OH + \frac{1}{2}H_2 \tag{18}$$

and

$$\overline{S}^0_{OH} = \Delta\overline{S}^0_{OH_{ads}/H_2} - \frac{1}{2}\overline{S}^0_{H_2} + S^0_{H_2O} \tag{19}$$

Table 1 summarizes the results obtained for hydrogen and OH adsorption on Pt(111) through this approach. For these calculations, $\overline{S}^0_{H_2} = 69.8\text{J/molK}$ and $\overline{S}^0_{H_2O} = 69.8\text{J/molK}$ were taken [121].

From these values and a model based on simple statistical thermodynamic considerations, the entropy of the adsorbed species as a function of the coverage can be calculated and compared with the entropy of a fully mobile or immobile adlayer, in order to gain some knowledge about the mobility of the adsorbed species.

A second approach to analyse the dependence with the temperature of the voltammetry of platinum electrodes is that based on the electrocapillary equation [111, 126, 127]. This approach overcomes the limitation imposed by the assumption about the shape of the isotherm. It can be demonstrated that the electrocapillary equation can be written, for platinum electrodes, in the following way [126]:

$$-d\gamma = Q d\Delta^M_S\phi - \frac{Q}{F}d\mu_{e^-} + (\Gamma_H + \Gamma_{H^+} - \Gamma_{OH} - \Gamma_{OH^-})d\mu_{H^+} + \sum_{i\neq e^-,H^+,OH^-,H_2O,M} \Gamma_i d\mu_i + \Gamma_S dT - \Gamma_V dp \tag{20}$$

where Γ_S and Γ_V are the relative entropy and volume per unit area of the interphase, respectively; T is the absolute temperature and p is the pressure. As before, the important point to realize is that the extension of the electrocapillary equation requires the introduction of the concept of the total charge, Q. In Eq. 20, the reference electrode has not been introduced and the differential of the chemical potential of electrons in the electrode is not zero because we are now considering a differential change of temperature and

$$\left(\frac{\partial\mu_i}{\partial T}\right)_{p,n_i} = -\overline{S}_i \tag{21}$$

Table 1 Standard entropy change for the hydrogen and hydroxyl adsorption reaction on Pt(111), $\Delta\overline{S}^0_{i/H_2}$, according to Eqs. 14 and 18 and standard entropy of the adsorbed species, $\overline{S}^0_i$

	$\Delta\overline{S}^0_{i/H_2}$/J mol^{-1} K^{-1}	$\overline{S}^0_i$/J mol^{-1} K^{-1}
H	−51	14
OH	−37	−32

where $\overline{S}_i$ is the molar entropy of compound i. Because the chemical potential also depends on the temperature, the total derivative of the surface tension vs the temperature differs from the interfacial entropy excess $\Gamma_S \neq \left(\frac{\partial\gamma}{\partial T}\right)_{p,n_i}$ and a new magnitude should be defined, namely the entropy of formation of the double layer.

$$\Delta S = \Gamma_S + \frac{Q}{F}\overline{S}_{e^-} - (\Gamma_H + \Gamma_{H^+} - \Gamma_{OH} - \Gamma_{OH^-})\overline{S}_{H^+} - \sum_{i\neq e^-,H^+,OH^-,H_2O,M} \Gamma_i\overline{S}_i \tag{22}$$

In this way, the entropy of formation of the interphase, ΔS, is defined as the difference in entropy of the components of the interphase when they are forming part of it and when they are in the bulk of their respective phases [116]. With this definition and Eq. 20,

$$\left(\frac{\partial\Delta S}{\partial Q}\right)_{T,p,a_i} = -\left(\frac{\partial\Delta^M_S\phi}{\partial T}\right)_{Q,p,a_i} \tag{23}$$

From this, the molar entropy of adsorbed species can be calculated. If double layer effects are neglected (or corrected with the use of the laser perturbation technique described below):

$$\Delta S = \Gamma_H\Delta\overline{S}_H + \Gamma_{OH}\Delta\overline{S}_{OH}$$

where $\Delta\overline{S}_H$ and $\Delta\overline{S}_{OH}$ are the molar entropies involved in the adsorption reactions:

$$\Delta\overline{S}_H = \overline{S}^{ads}_H - \overline{S}_{H^+} - \overline{S}_{e^-} \tag{24}$$

$$\Delta\overline{S}_{OH} = \overline{S}^{ads}_{OH} - \overline{S}_{H_2O} + \overline{S}_{H^+} + \overline{S}_{e^-} \tag{25}$$

From these, the entropies of the adsorbed species can be calculated. In this case, the tabulated value of the entropy of proton in solution, $S_{H^+} = 3.5\,\text{J/molK}$, can be used. The entropy of electrons is taken as zero for the Fermi–Dirac electron gas [121]. Results obtained from the method based on the generalized isotherm and those obtained from the analysis based on the electrocapillary equation just described are compared in Fig. 12. A general agreement is observed between both methods. More importantly, the entropy of adsorbed hydrogen lies very close to the values obtained for a fully mobile adlayer, indicating that adsorbed hydrogen on Pt(111) possess very high surface diffusion velocity. On the contrary, the entropy of adsorbed OH is rather low, closer to the values of the immobile adlayer.

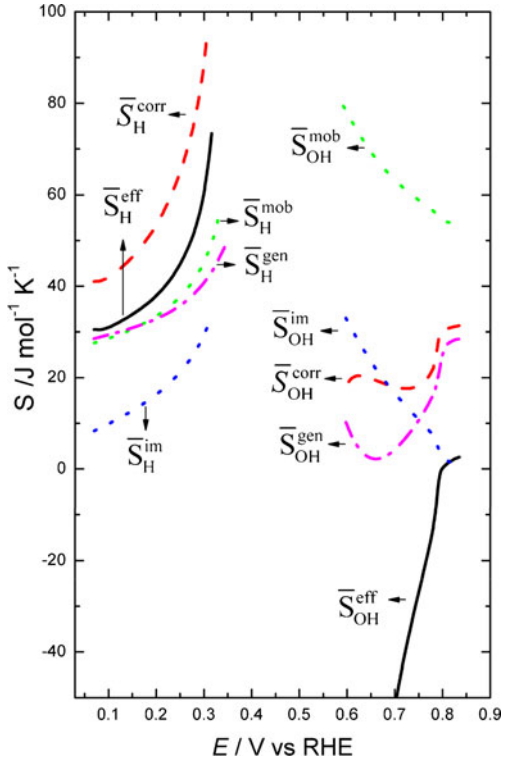

Fig. 12 Absolute entropies of adsorbed hydrogen and OH species, as evaluated by different approximations (reprinted with permission from Garcia-Araez et al. [126])

Laser-induced temperature jump method

An alternative approach to study the effect of the temperature on the electrochemical double layer was also initially proposed and applied to mercury electrodes [128]. In this method, a high power laser is directed to the surface of the electrode. The wavelength of the radiation is chosen in such a way that its only effect is to heat the interphase. By using a high power pulsed laser, it is possible with this method to raise the temperature of the interphase by several degrees in the submicrosecond time scale [128–135]. For sufficiently fast processes, the coulostatic change of the potential that takes place in response to this change of the temperature contains important thermodynamic information, in particular, about the entropy of formation of the interphase. If slow processes take place, the technique becomes a relaxation method for the investigation of the kinetics of the process [130, 136]. The application of this approach to study mercury or gold electrodes does not offer much advantage in comparison with the much more simple use of a thermostatic bath to change the temperature of the whole working solution. However, this method has proved very valuable to obtain novel information for platinum single crystal electrodes. This is because the fast perturbation of the temperature allows separation of the response from the pure double layer from that resulting from the hydrogen and anion adsorption processes [130]. By appropriate selection of the experimental conditions, specially the pH of the solution, adsorption processes become much slower than the double layer response and the coulostatic potentials transients contain only information about the double layer. In this way, the following thermal coefficient can be obtained: $\left(\partial \Delta_S^M \phi / \partial T\right)_{\sigma_M, \Gamma_H, \Gamma_{OH}, p, a_i}$. (cf. right hand side of Eq. 23). The subindex in the previous partial derivative indicates that the temperature variation has been done so fast that the coverage of adsorbed species is kept constant in a frozen state. In other words, only the

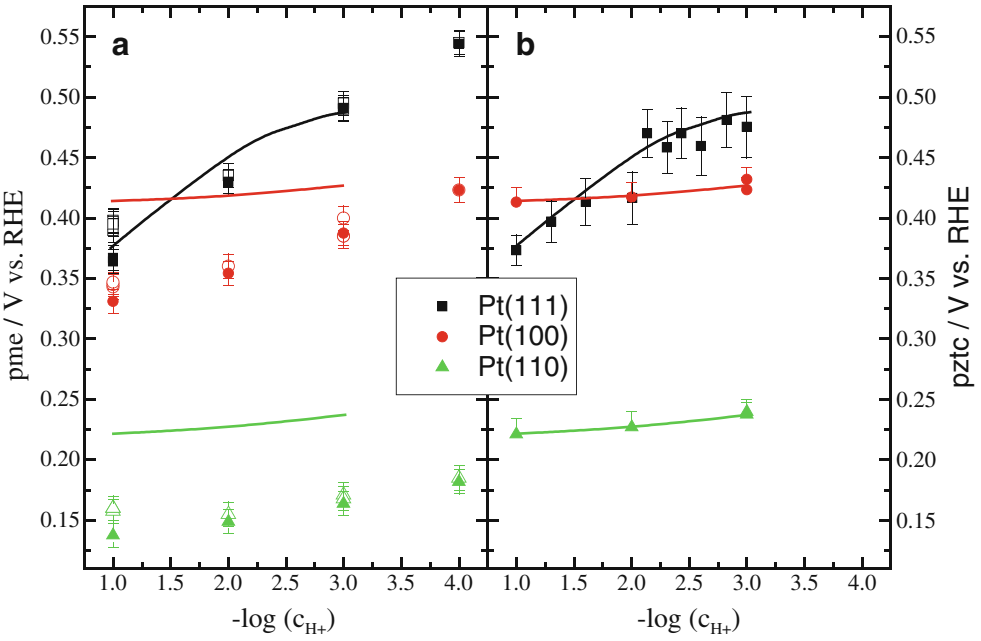

Fig. 13 Values of **a** pmes, uncorrected (*open symbols*) and corrected (*filled symbols*) from the thermodiffusion potential and **b** pztcs, for Pt(111), Pt(100) and Pt(110) electrodes in $(0.1-x)$M $KClO_4$+xM $HClO_4$ solutions. *Lines* are drawn to indicate the tendencies of pztc values, and they are reproduced in the *left figure* in order to facilitate the comparison with pme values (reprinted with permission from Garcia-Araez et al. [135])

double layer is responding to the perturbation. This coefficient has been used to correct double layer contributions to the entropy of adsorbed species shown in Fig. 12. This response is dominated by the reorganization of solvent molecules in the interphase. It has been shown that the sign of this coefficient provides evidence on the net orientation of the water at the interphase. A negative coefficient indicates water oriented with the hydrogen towards the metal while a positive coefficient indicates water oriented with oxygen towards the metal. The particular potential where the coefficient change sign coincides with a net orientation of the water parallel to the surface and, according to Eq. 23 (more precisely with a variation of Eq. 23 that involves only double layer processes), with the potential of maximum entropy of double layer formation (pme). If only electrostatic interaction dominated the orientation of water at the interphase, the pme would coincide with the pzfc. However, a specific interaction between water and the metallic surface could lead to different values of these magnitudes.

Unfortunately, the pzfc is an elusive non-thermodynamic magnitude, and therefore, it is difficult to make the comparison between pzfc and pme. Only for Pt(111) an estimation of the pzfc can be given. The more recent estimations locate the pztc of Pt(111) within the double layer region [84, 135]. In this case, since no adsorption processes take place in this potential range, pzfc and pztc become identical. Moreover, the pme is located very close to the latter, indicating that indeed electrostatic interactions dominate the orientation of water. The location of the pztc and pme are compared in Fig. 13. It can be seen that, while for Pt(111) they lie very close, for Pt(100) and Pt(110), the pme is located at a lower potential than the pztc. This can be taken as an indication that the pzfc is also located at lower potentials than the pztc, in agreement with the historical results reported for polycrystalline platinum by A.N. Frumkin and Petrii [137].

Concluding remarks

In this work, we have tried to provide, from an historical perspective, an overview of the present situation about the understanding of platinum electrochemistry. The strong dependence of the electrochemical behaviour on the crystallographic structure implies that careful methodologies for the preparation and characterisation of platinum surfaces are necessary if well-defined and reproducible data are sought. We showed above that detailed interfacial information has been gathered about the electrochemical the reactivity of platinum in the last three decades. This information will be undoubtedly very important to approach both fundamental and applied problems regarding platinum electrochemistry. At a fundamental level, we could say that the time is now ripe for theoretical studies addressing the properties of platinum surfaces in electrochemical environment. At this level, it is crucial to have experimental data to compare with theoretical calculations that has been obtained under very well-defined and reproducible conditions. The knowledge gathered with platinum single crystal is also valuable for applied investigations. In this regard, the possibility of preparing nanoparticles with defined surface structures [138] can be seen as filling the gap between the fundamental studies with platinum single crystal and the applied research in electrocatalysis. Finally, we want to stress the importance of the properties mentioned above, such as the pztc, pzfc and the pme, energies and entropies of adsorption and orientation of adsorbed water as key properties giving clues to understand the reactivity of platinum with unprecedented detail.

Acknowledgements Financial support from the Ministerio de Educación y Ciencia of Spain through the project CTQ2010-16271 (Feder) and Generalitat Valenciana (Feder) through PROMETEO/2009/045 project is thankfully acknowledged.

References

1. Somorjai GA (1994) Introduction to surface chemistry and catalysis. Wiley, New York
2. Angerstein-Kozlowska H, Conway BE, Sharp WBA (1973) J Electroanal Chem 43(1):9–36
3. Conway BE, Angerstein-Kozlowska H, Sharp WBA, Criddle EE (1973) Anal Chem 45(8):1331–1336
4. Woods R (1974) J Electroanal Chem 49(2):217–226
5. Breiter MW (1962) Electrochim Acta 8(12):925–935
6. Trasatti S, Petrii OA (1991) Pure Appl Chem 63:711–734
7. Breiter MW (1964) J Electroanal Chem 8(6):449
8. Kolb DM (1978) In: Gerischer H, Tobias CW (eds) Advances in electrochemistry and electrochemical engineering, vol 11, ch 2. Wiley-Interscience, New York, p 125
9. Angerstein-Kozlowska H, Conway BE, Barnett B, Mozota J (1979) J Electroanal Chem 100(1–2):417–446
10. Conway BE (1995) Prog Surf Sci 49(Iss 4):331–452
11. Will FG (1965) J Electrochem Soc 112(4):451–455
12. Ishikawa RM, Hubbard AT (1976) J Electroanal Chem 69 (3):317–338
13. O'Grady WE, Woo MYC, Hagans PL, Yeager E (1977) J Vac Sci Technol 14(1):365–368
14. Hubbard AT, Ishikawa R, Katekaru J (1978) J Electroanal Chem 86(2):271–288
15. Yeager E, Homa A, Cahan BD, Scherson D (1982) J Vac Sci Technol 20(3):628–633
16. Homa AS, Yeager E, Cahan BD (1983) J Electroanal Chem 150:181–192
17. Ross PN (1979) J Electrochem Soc 126(1):67–77
18. Ross Jr (1981) Surf Sci 102(2–3):463–485
19. Dickertmann D, Koppitz FD, Schultze JW (1976) Electrochim Acta 21(11):967–971
20. Clavilier J, Faure R, Guinet G, Durand R (1980) J Electroanal Chem 107:205–209
21. Clavilier J (1980) J Electroanal Chem 107:211–216
22. Clavilier J, Durand R, Guinet G, Faure R (1981) J Electroanal Chem 127:281

23. Clavilier J, Armand D, Wu BL (1982) J Electroanal Chem 135:159–166
24. Motoo S, Furuya N (1984) J Electroanal Chem 172:339–358
25. Wagner FT, Ross PN (1983) J Electroanal Chem 150:141–164
26. Scortichini CL, Reilley CN (1982) J Electroanal Chem 139:233–245
27. Scortichini CL, Reilley CN (1982) J Electroanal Chem 139:247–264
28. Scortichini CL, Woodward FE, Reilley CN (1982) J Electroanal Chem 139:265–274
29. Arvia AJ, Canullo JC, Custidiano E, Perdriel CL, Triaca WE (1986) Electrochim Acta 31(11):1359–1368
30. Arvia AJ, Salvarezza RC, Triaca WE (1989) Electrochim Acta 34(8):1057–1071
31. Aberdam D, Durand R, Faure R, ElOmar F (1986) Surf Sci 171 (2):303–330
32. Feddrix FH, Yeager EB, Cahan BD (1992) J Electroanal Chem 330(1–2):419–431
33. Wasberg M, Palaikis L, Wallen S, Kamrath M, Wieckowski A (1988) J Electroanal Chem 256(1):51–63
34. Zurawski D, Rice L, Hourani M, Wieckowski A (1987) J Electroanal Chem 230(1–2):221–231
35. Wagner FT, Ross PN (1988) J Electroanal Chem 250:301–320
36. Motoo S, Furuya N (1987) Ber Bunsenges Phys Chem 91:457–461
37. Clavilier J, El Achi K, Rodes A (1989) J Electroanal Chem 272:253–261
38. Rodes A, El Achi K, Zamakhchari MA, Clavilier J (1990) J Electroanal Chem 284:245–253
39. Clavilier J, El Achi K, Rodes A (1990) Chem Phys 141:1–14
40. Markovic NM, Marinkovic NS, Adzic RR (1988) J Electroanal Chem 241:309–328
41. Itaya K, Sugawara S, Sashikata K, Furuya N (1990) J Vac Sci Technol, A 8:515–519
42. Clavilier J (1982) In: Paper IA11 presented at the 33th meeting of the International Society of Electrochemistry, Lyon, France
43. Zei MS, Batina N, Kolb DM (1994) Surf Sci Lett 306:L519–L528
44. Furuya N, Shibata M (1999) J Electroanal Chem 467(1–2):85–91
45. Furuya N, Ichinose M, Shibata M (1999) J Electroanal Chem 460(1–2):251–253
46. Clavilier J, Orts JM, Feliu JM (1994) J Phys IV 4:1–303
47. Feliu JM, Rodes A, Orts JM, Clavilier J (1994) Pol J Chem 68:1575–1595
48. Kibler LA, Cuesta A, Kleinert M, Kolb DM (2000) J Electroanal Chem 484:73–82
49. Herrero E, Orts JM, Aldaz A, Feliu JM (1999) Surf Sci 440:259–270
50. Samjeske G, Xiao XY, Baltruschat H (2002) Langmuir 18 (12):4659–4666
51. Al-Akl A, Attard GA, Price R, Timothy B (1999) J Electroanal Chem 467(1–2):60–66
52. Al-Akl A, Attard G, Price R, Timothy B (2001) Phys Chem Chem Phys 3(16):3261–3268
53. Souza-Garcia J, Climent V, Feliu JM (2009) Electrochem Commun 11(7):1515–1518
54. Titmuss S, Wander D, King DA (1996) Chem Rev 96:1291–1305
55. Lucas CA, Markovic NM, Ross PN (1996) Phys Rev Lett 77 (24):4922–4925
56. Michaelis R, Kolb DM (1992) J Electroanal Chem 328:341–348
57. Clavilier J, Rodes A (1993) J Electroanal Chem 348(1–2):247–264
58. Huxter SE, Attard GA (2006) Electrochem Commun 8 (11):1806–1810
59. El-Aziz AM, Hoyer R, Kibler LA (2010) Chemphyschem 11 (13):2906–2911
60. Xu QQ, Linke U, Bujak R, Wandlowski T (2009) Electrochim Acta 54(23):5509–5521
61. Wen R, Lahiri A, Alagurajan M, Kuzume A, Kobayashi S, Itaya K (2010) J Electroanal Chem 649(1–2):257–260
62. Wen R, Lahiri A, Azhagurajan M, Kobayashi S, Itaya K (2010) J Am Chem Soc 132(39):13657–13659
63. Clavilier J, Rodes A, El Achi K, Zamakhchari MA (1991) J Chim Phys 88(7–8):1291–1337
64. Al Jaaf-Golze K, Kolb DM, Scherson DA (1986) J Electroanal Chem 200:353–362
65. Nart FC, Iwasita T, Weber M (1994) Electrochim Acta 39:961
66. Berna A, Feliu JM, Gancs L, Mukerjee S (2008) Electrochem Commun 10(11):1695–1698
67. Wieckowski A, Zelenay P, Varga K (1991) J Chim Phys 88(7–8):1247–1270
68. Kolics A, Wieckowski A (2001) J Phys Chem B 105(13):2588–2595
69. Sawatari Y, Inukai J, Ito M (1993) JElectron SpectroscRelatPh 64–65:515
70. Ogasawara H, Sawatari Y, Inukai J, Ito M (1993) J Electroanal Chem 358:337
71. Faguy PW, Markovic N, Adzic RR, Fierro CA, Yeager E (1990) J Electroanal Chem 289:245
72. Faguy PW, Marinkovic NS, Adzic RR (1996) Langmuir 12 (2):243–247
73. Faguy PW, Marinkovic NS, Adzic RR (1996) J Electroanal Chem 407(Iss 1–2):209–218
74. Lachenwitzer A, Li N, Lipkowski J (2002) J Electroanal Chem 532(1–2):85–98
75. Clavilier J, Albalat R, Gómez R, Orts JM, Feliu JM, Aldaz A (1992) J Electroanal Chem 330:489–497
76. Clavilier J, Orts JM, Gómez R, Feliu JM, Aldaz A (1994) In: Conway BE, Jerkiewicz G (eds) The Electrochemical Society Proceedings, vol 94–21. The Electrochemical Society, Pennington, pp 167–183
77. Feliu JM, Orts JM, Gómez R, Aldaz A, Clavilier J (1994) J Electroanal Chem 372:265–268
78. Orts JM, Gómez R, Feliu JM, Aldaz A, Clavilier J (1994) Electrochim Acta 39(11/12):1519–1524
79. Herrero E, Feliu JM, Wieckowski A, Clavilier J (1995) Surf Sci 325:131–138
80. Climent V, Gómez R, Feliu JM (1999) Electrochim Acta 45(4–5):629–637
81. Climent V, Gómez R, Orts JM, Aldaz A, Feliu JM (2000) In: Jerkiewicz G, Feliu JM, Popov BN (eds) The Electrochemistry Society Proceedings (Hydrogen at Surfaces and Interfaces), vol 2000–16. The Electrochemical Society, Pennington, pp 12–30
82. Gómez R, Feliu JM, Aldaz A, Weaver MJ (1998) Surf Sci 410 (1):48–61
83. Rodes A, Climent V, Orts JM, Pérez JM, Aldaz A (1998) Electrochim Acta 44(6–7):1077–1090
84. Climent V, Garcia-Araez N, Herrero E, Feliu JM (2006) Russ J Electrochem 42:1145–1160
85. Clavilier J, Orts JM, Gómez R, Feliu JM, Aldaz A (1996) J Electroanal Chem 404(2):281–289
86. Orts JM, Gómez R, Feliu JM, Aldaz A, Clavilier J (1997) Langmuir 13(11):3016–3023
87. Chen QS, Solla-Gullon J, Sun SG, Feliu JM (2010) Electrochim Acta 55(27):7982–7994
88. Grahame DC (1947) Chem Rev 41:441–501
89. Lipkowski J, Schmickler W, Kolb DM, Parsons R (1998) J Electroanal Chem 452(2):193–197
90. Frumkin AN, Petrii OA, Damaskin BB (1980) In: Bockris JOM, Conway BE, Yeager E (eds) Comprehensive treatise of electrochemistry, vol 1. Plenum, New York, pp 221–289
91. Savich W, Sun SG, Lipkowski J, Wieckowski A (1995) J Electroanal Chem 388(Iss 1–2):233–237

92. Mostany J, Herrero E, Feliu JM, Lipkowski J (2002) J Phys Chem B 106(49):12787–12796
93. Herrero E, Mostany J, Feliu JM, Lipkowski J (2002) J Electroanal Chem 534(1):79–89
94. Mostany J, Herrero E, Feliu JM, Lipkowski J (2003) J Electroanal Chem 558:19–24
95. Mostany J, Martinez P, Climent V, Herrero E, Feliu JM (2009) Electrochim Acta 54(24):5836–5843
96. Garcia-Araez N, Climent V, Herrero E, Feliu J, Lipkowski J (2005) J Electroanal Chem 576(1):33–41
97. Garcia-Araez N, Climent V, Herrero E, Feliu JM, Lipkowski J (2005) J Electroanal Chem 582(1–2):76–84
98. Garcia-Araez N, Climent V, Herrero E, Feliu J, Lipkowski J (2006) J Electroanal Chem 591(2):149–158
99. Garcia-Araez N, Climent V, Herrero E, Feliu JM, Lipkowski J (2006) Electrochim Acta 51(18):3787–3793
100. Garcia-Araez N, Climent V, Rodriguez P, Feliu JM (2008) Electrochim Acta 53(23):6793–6806
101. Garcia-Araez N, Climent V, Rodriguez P, Feliu JM (2010) Langmuir 26(14):12408–12417
102. Garcia-Araez N, Climent V, Rodriguez P, Feliu JM (2010) Phys Chem Chem Phys 12(38):12146–12152
103. Su Z, Climent V, Leitch J, Zamlynny V, Feliu JM, Lipkowski J (2010) Phys Chem Chem Phys 12(46):15231–15239
104. Funtikov AM, Stimming U, Vogel R (1997) J Electroanal Chem 428(1–2):147–153
105. Braunschweig B, Daum W (2009) Langmuir 25(18):11112–11120
106. Edens GJ, Gao X, Weaver MJ (1994) J Electroanal Chem 375:357–366
107. Wan LJ, Suzuki T, Sashikata K, Okada J, Inukai J, Itaya K (2000) J Electroanal Chem 484(2):189–193
108. Kim YG, Soriaga JB, Vigh G, Soriaga MP (2000) J Colloid Interface Sci 227:505–509
109. Wan LJ, Yau SL, Itaya K (1995) J Phys Chem 99(Iss 23):9507–9513
110. Garcia N, Climent V, Orts JM, Feliu JM, Aldaz A (2004) Chemphyschem 5:1221–1227
111. Garcia-Araez N, Climent V, Feliu JM (2008) J Solid State Electrochem 12(4):387–398
112. Braunschweig B, Mukherjee P, Dlott DD, Wieckowski A (2010) J Am Chem Soc 132(40):14036–14038
113. Hills GJ, Payne R (1965) Trans Faraday Soc 61(2):326–349
114. Hills G (1969) J Phys Chem 73(11):3591–3597
115. Hills GJ, Hsieh S (1975) J Electroanal Chem 58(1):289–298
116. Harrison JA, Randles JEB, Schiffrin DJ (1973) J Electroanal Chem 48(3):359–381
117. Hamelin A, Stoicoviciu L, Silva F (1987) J Electroanal Chem 229(1–2):107–124
118. Hamelin A, Stoicoviciu L, Silva F (1987) J Electroanal Chem 236(1–2):283–294
119. Silva F, Sottomayor MJ, Hamelin A, Stoicoviciu L (1990) J Electroanal Chem 295(1–2):301–316
120. Silva F, Sottomayor MJ, Hamelin A (1990) J Electroanal Chem 294(1–2):239–251
121. Conway BE, Angerstein-Kozlowska H, Sharp WB (1978) J Chem Soc Faraday Trans 74(6):1373–1389
122. Zolfaghari A, Jerkiewicz G (1997) J Electroanal Chem 422(1–2):1–6
123. Zolfaghari A, Jerkiewicz G (1997) J Electroanal Chem 420(1–2):11–15
124. Zolfaghari A, Jerkiewicz G (1999) J Electroanal Chem 467(1–2):177–185
125. Radovic-Hrapovic Z, Jerkiewicz G (2001) J Electroanal Chem 499(1):61–66
126. Garcia-Araez N, Climent V, Feliu J (2009) J Phys Chem C 113 (46):19913–19925
127. Garcia-Araez N, Climent V, Feliu JM (2010) J Electroanal Chem 649(1–2):69–82
128. Benderskii VA, Velichko GI (1982) J Electroanal Chem 140(1):1–22
129. Climent V, Coles BA, Compton RG (2002) J Phys Chem B 106:5258–5265
130. Climent V, Coles BA, Compton RG (2002) J Phys Chem B 106:5988–5996
131. Climent V, Coles BA, Compton RG, Feliu JM (2004) J Electroanal Chem 561:157–165
132. Climent V, Garcia-Araez N, Compton RG, Feliu JM (2006) J Phys Chem B 110(42):21092–21100
133. Garcia-Araez N, Climent V, Feliu JM (2008) J Am Chem Soc 130(12):3824–3833
134. Garcia-Araez N, Climent V, Feliu JM (2009) Electrochim Acta 54(3):966–977
135. Garcia-Araez N, Climent V, Feliu J (2009) J Phys Chem C 113 (21):9290–9304
136. Smalley JF, Krishnan CV, Goldman M, Feldberg SW, Ruzic I (1988) J Electroanal Chem 248(2):255–282
137. Frumkin AN, Petrii OA (1975) Electrochim Acta 20:347–359
138. Solla-Gullon J, Rodriguez P, Herrero E, Aldaz A, Feliu JM (2008) Phys Chem Chem Phys 10(10):1359–1373